

Detecting Abnormal Cell Division Patterns in Early Stage Human Embryo Development

Aisha Khan¹(✉), Stephen Gould¹, and Mathieu Salzmann^{1,2,3}

¹ College of Engineering and Computer Science,
The Australian National University, Canberra, Australia
`aisha.khan@anu.edu.au`

² Computer Vision Research Group, NICTA, Canberra, Australia

³ CVLab, EPFL, Lausanne, Switzerland

Abstract. Recently, it has been shown that early division patterns, such as cell division timing biomarkers, are crucial to predict human embryo viability. Precise and accurate measurement of these markers requires cell lineage analysis to identify normal and abnormal division patterns. However, current approaches to early-stage embryo analysis only focus on estimating the number of cells and their locations, thus failing to detect abnormal division patterns and potentially yielding incorrect timing biomarkers. In this work we propose an automated tool that can perform lineage tree analysis up to the 5-cell stage, which is sufficient to accurately compute all the known important biomarkers. To this end, we introduce a CRF-based cell localization framework. We demonstrate the benefits of our approach on a data set of 22 human embryos, resulting in correct identification of all abnormal division patterns in the data set.

1 Introduction

Predicting human embryo viability is one of the most relevant aspects of Assisted Reproductive Technology such as *in vitro* fertilization (IVF). Despite considerable research effort IVF have stagnant and unsatisfactory low success rate [2]. This is mainly due to little understanding of the basic biological aspects of early human embryo development, including factors that would aid in predicting successful development. In most cases embryologists assess embryo viability subjectively based on few visual observations, and critical events between observations may go unnoticed. Furthermore, embryo development is a complex process in which the exact timing and sequence of events are as essential as the successful completion of the events themselves. This requires continuous monitoring of each developing embryo and reliable embryo assessment biomarkers [2].

Recent advances in time-lapse microscopy has led to the study of the dynamics of developing embryos, and results in more reliable non-invasive embryo viability markers. A set of timing markers reported by Wong et al. [13] have been confirmed to be highly indicative of subsequent viability of the embryo [2]. These

We are grateful to Auxogyn, Inc. for their valuable support of this project.

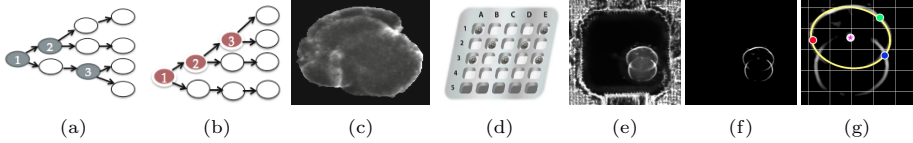


Fig. 1. Example of normal (a) and abnormal (b) division patterns. (c) Example of a 5-cell stage frame. (d) Petri Dish. (e) Raw image. (f) Hessian image. The Hessian image is used for proposing cell candidates by ellipse fitting (g).

markers are: (i) the duration of the first cleavage furrow from the beginning to the appearance of two cells; (ii) the duration of the 2-cell stage; and (iii) the time between the cleavage of each of the two cells to their respective daughter cells in the 4-cell stage. Recently, an additional timing parameter was proposed to complement the above-mentioned three parameters: (iv) the time to reach the 5-cell stage [9].

Current approaches [4, 5, 10, 12, 13] measure these timing parameters by performing cell detection and localization and ignore cell lineage. But cell lineage is vital for accurate measurement of the third timing parameter that requires identification of abnormal division patterns. Embryos can follow different courses of divisions after the first division (two cell stage). For the purpose of this study, a division pattern is considered normal when each of the cells at the 2-cell stage further divides to reach the 4-cell stage and is considered abnormal when only one of the two cells further divides to reach the 4-cell stage (see Fig. 1(a)–(b)). Two embryos classified to be at the same developmental stage (i.e., four cells) can be a product of completely different developmental processes. Since current approaches ignore lineage, they are unable to identify the cause of abnormal division patterns resulting in invalid timing measurements.

In this work, we introduce an approach that identifies abnormal division patterns in early stage human embryo development and allows accurate and precise measurements of timing parameters to be fully automated. Our approach allows embryologists to make use of detailed measurements that resolve cell ancestry. Manual characterization of the lineage requires biologist to maintain a rigorous observation regime and can also be prone to high inter-observer and intra-observer variability. This poses a huge hurdle for practical clinical implementation. By contrast, automated measurement of these tasks can alleviate this burden and may provide an objective, standardized embryo quality assessment free of human biases.

Our approach can be applied to any model that performs localization of individual cells. However, current models are limited to the 4-cell stage (e.g., [5, 10]). Here, we therefore introduce a model that localizes cells beyond the 4-cell stage. We demonstrate the effectiveness of our model to detect and localize cells, and to trace their lineage in challenging microscopy images of developing human embryos. This allows us to identify abnormal cell division patterns and correctly assign timing parameters.

Related Work. Many authors have cited the complexities of monitoring human embryo development [4, 5, 10], which makes many of the standard detection, segmentation and tracking techniques not feasible (see Fig. 1(c) for an example of large overlap and poor visual features in the 5-cell stage). While some techniques have been proposed to detect cell divisions and perform cell tracking in microscopic images in general [3, 7, 8, 11, 14] and of embryos in particular [1, 6], they typically require the cells to be stained, and thus cannot realistically be applied to human embryonic cells in an in vitro fertilization setting.

In the context of human embryonic cells, recent efforts have been made to automate the monitoring of early stage embryo development in an attempt to measure the timing parameters defined above. For example, Wang et al. [12] proposed a 3-level classification method to predict the embryo cell stage without explicit segmentation and tracking. However, our goal is to detect cell divisions by localizing and tracking cells to aid the biologists in the discovery and characterization of novel biological phenomena. Subsequently, a traditional particle filter based approach was proposed to detect cell divisions [13]. However, in the context of tracking multiple deforming objects, such as human embryos, traditional particle filters face problems due to the high dimensional search space. Similarly, Moussavi et al. [10] proposed a method to detect cell divisions by simultaneous segmentation and tracking cell boundaries in a conditional random field (CRF). However, the segmentation label space grows exponentially with number of cells and segments. Subsequently, a linear chain Markov model was proposed to detect and localize cells [5]. Their method uses cell spatial information along with a spatial continuity enforcement constraint, but suffers from label space exponential growth with the number of cells. The label space growth limits these models to the 4-cell stage. Moreover, these approaches detect cell divisions by tracking cell boundary between frames only, and no lineage tree analysis is performed. Importantly, all these methods are limited to the 4-cell stage, and measurement of timing parameters beyond four cells can only be performed manually.

While Khan et al. [4] recently proposed a method to identify the number of cells in an image up to five cells, their approach does neither localize the cells, nor track them. Furthermore, existing methods that construct lineage trees [1, 3, 6, 7, 11] have only been applied to stained cells with clear division patterns. As such, they are unable to handle the complexity of non-stained human embryos. In short, there exist no methods that can accurately measure the timing parameters of early-stage human embryo development and identify aberrant division patterns. In this work, we propose a CRF based model that identifies abnormal cell divisions by detecting and tracking individual cells. This allows accurate measurement of embryo viability markers and also provides biologists with detailed information about the developing embryo.

2 Methodology

Our goal is to monitor the patterns of cell division in microscopy images of evolving embryos. We achieve this by performing lineage tree analysis over the

complete image sequence. Given cell location information for each of the cells within a frame our approach generates a complete ancestry by associating daughters to their mother in the previous frame. Importantly, our method can be applied to any system that outputs cell localization information.

Lineage Tree Construction. We propose to model the cell division ancestry as a lineage tree. To this end, and for the time being, let us assume that we are given the number of cells and their locations in a sequence of microscopy images. Our approach generates a lineage tree by associating each cell in a frame to its mother in the previous frame. If a cell is dividing, it is called a mother cell, and its two daughter cells share the same mother. Between consecutive frames, cell shape and location change in a confined manner. When a cell divides, its two daughters are almost half the size of their mother and, combined, present a similar shape to that of the mother. Using this fact, we associate cells between adjacent frames with highest intersection over union (IoU) between them. The IoU is computed by measuring the area of intersection of the two ellipses—one in each frame—divided by the area of their union.

Formally, let x^t and x^{t+1} denote the set of cells in the embryo at frames t and $t+1$, respectively. Then, an association between cells at frames t and $t+1$ is defined as

$$a^* = \operatorname{argmin}_a \sum_{c \in x^{t+1}} \gamma(c, a(c)) \quad (1)$$

where $c \in x^{t+1}$ and $a(\cdot)$ is the association mapping from daughter to mother, where $a(c)$ returns the cell in x^t associated with cell c . To ensure a valid association, the following constraints are enforced; (i) each cell in frame $t + 1$ must have at most one mother; and (ii) each cell in frame t can either be assigned to a unique cell candidate in next frame or can divide and be associated with two or more cell candidates in the next time frame. The function γ measures the affinity of mapping c to $a(c)$ by computing the IoU between c and $a(c)$.

The lineage tree over the entire sequence can be obtained by finding a^* between all consecutive frames. Since this only requires the locations of the cells, it can be applied to any existing cell localization method. However, existing methods are limited to the 4-cell stage, which is insufficient to obtain the last timing parameter (i.e., time to reach the 5-cell stage). Therefore, here, we introduce a new cell localization approach that can track the embryo beyond the 4-cell stage.

Cell Localization Model. Our model predicts the numbers and locations of the cells over time. We pose this problem in a CRF framework. We begin by pre-processing the images to produce a set of ellipses representing candidate cells within the image. The candidates define the label space for each time slice in our model. We infer the most likely number and location of cells for each frame with efficient exact inference.

Images of the developing embryos are captured by the *Eeva*TM System developed by Auxogyn, Inc. Embryos are placed in a petri dish inside the incubator

where images are taken at 5-minute intervals over a three to five day period. Our method generates elliptical cell candidates for each frame using randomized sampling in conjunction with ellipse fitting [5]. This results in a small set of candidates (e.g., 100), which comprises the label space. Different frames have different label spaces as these are generated from evidence within each image (see Fig. 1 (d)–(g)).

We wish to annotate each frame in the image with the number and location of all cells within that frame. We formulate this by representing an embryo’s state at time t by a set of variables. Let N_{max} be the maximum number of cells that can be predicted from the embryo’s morphology (e.g., five). The variables are the number of cells $N^t \in \{1, 2, \dots, N_{max}\}$, and cell location variables Y_m^t , one per cell, $m \in \{1, 2, \dots, N_{max}\}$. Each location variable Y_m^t can take on a label from the label space $\mathbf{L}^t = \{c_1^t, \dots, c_K^t, d^t\}$ corresponding to the K candidates, described above, and a special dummy label d^t , which allows us to account for frames containing less than N_{max} cells, and thus corresponding location variables should not be assigned a candidate. In a fully connected inter-slice graph we define four compatibility functions over the variables within one time slice: (i) a classifier probability on N^t (Φ_1); (ii) a unary potential over Y^t (Φ_2); (iii) a compatibility function between Y_m^t and N^t (Φ_3); and (iv) a similarity constraint on Y^t (Φ_4).

The function Φ_1 provides a prediction on N^t from the intensity images [4]. Briefly, a linear chain Markov model is applied on intensity images with learned unary and pairwise potentials to predict the number of cells directly in an image. The framework takes the feature vector of a frame as input, and returns a probability on the number of cells $p_N^t \in \mathbb{R}^{N_{max}}$. Then, the unary energy of the number of cells is equivalent to its negative log-probability.

Similarly, the function Φ_2 measures how much evidence there is for the candidate c^t in the image X^t . It is modeled as the output of a boosted decision tree classifier trained separately on a set of eight handcrafted and features extracted from the probability vector returned by Φ_1 . The classifier takes the feature vectors of candidates c^t for frame t as input, and returns a probability of labels \mathbf{L}^t for frame t . Then, we define Φ_2 as the negative log-probability of the boosted decision tree classifier.

The pairwise compatibility function Φ_3 between Y and N enforces that location variables $\{Y_i^t\}_{i=1, \dots, N^t}$ get a label from \mathbf{L}^t and the remaining location variables $\{Y_j^t\}_{j=N^t+1, \dots, N_{max}}$ get the dummy label d^t while the other variables don’t. The function is defined as

$$\Phi_3(Y_i^t, N^t) = \begin{cases} 0, & \text{if } (Y_i^t = d^t \wedge i > N^t) \vee (Y_i^t \neq d^t \wedge i \leq N^t) \\ \infty, & \text{otherwise.} \end{cases} \quad (2)$$

Function Φ_4 imposes a similarity constraint over Y^t such that no two location variables at time t represent the same part of the image. This is expressed as

$$\Phi_4(Y_i^t, Y_j^t, N^t) = \begin{cases} 0, & \text{if } \delta^t \leq \text{threshold}(N^t) \\ \infty, & \text{otherwise,} \end{cases} \quad (3)$$

where $\delta^t \in [0, 1]$ is a similarity measure between the candidates in label space \mathbf{L}^t defined in terms of IoU. This also imposes mutual exclusion constraints over Y^t . Here $\text{threshold}(N^t)$ is computed from training data by considering the IoU of all pairs of cell candidates (ellipses) close to the ground-truth (i.e., IoU w.r.t ground-truth ≥ 0.7) for each N^t separately. We set $\text{threshold}(N^t)$ as the 90-th percentile IoU.

We then seek to model the evolution of the cells over time by adding an inter-slice compatibility function. More specifically, we introduce a pairwise potential that scores the compatibility of labels, Y^t and Y^{t+1} , for two consecutive frames. Since we wish to capture cell division events we use a simple model that enforces the number of cells not to decrease from time t to time $t+1$. It also penalizes the case where a transition is skipped from time t to time $t+1$. This compatibility function is defined as

$$\psi_2^{t,t+1}(N^t, N^{t+1}) = \begin{cases} 0, & \text{if } (N^t = N^{t+1}) \vee (N^{t+1} = N^t + 1) \\ \infty, & \text{otherwise.} \end{cases} \quad (4)$$

We seek the most likely number of cells N^t and cell locations Y^t for each frame, and ultimately the most likely sequence. Formally, this corresponds to finding the variable configuration that minimizes the total CRF energy over all time frames, defined as

$$E(Y, N) = \sum_{t=1}^T \psi_1^t(Y_{\{1: N_{max}\}}^t, N^t) + \sum_{t=1}^{T-1} \psi_2^{t,t+1}(N^t, N^{t+1}), \quad (5)$$

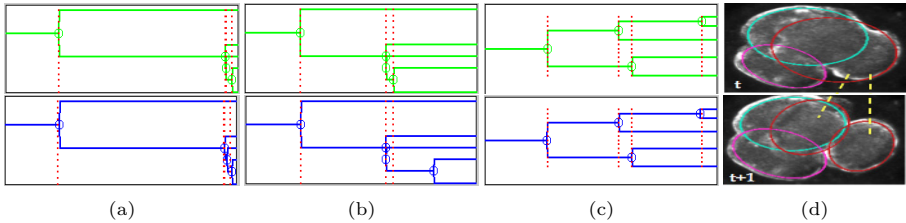
where $\psi_1^t(Y^t, N^t)$ is the sum of intra-slice compatibility functions defined above. We achieve this by performing exact inference using a junction tree within the time slice and belief propagation between time slices. Exact belief updating is then performed by message passing over the junction tree. This allows us to perform exact inference over long sequences. However, belief propagation over junction tree is known to be computationally intensive in the general case. Its complexity may increase dramatically with the connectivity and state space cardinality of the nodes. Exact inference became computationally hard with a large label space ($K > 30$) for $N_{max} = 5$. So in that case we applied max-product approximate inference within a time slice.

3 Experiments

We evaluated our approach on 22 developing embryos from eight different patients, consisting of a total of 9260 frames with 71 cell divisions. Ground truth for these sequences was generated by manually annotating each cell division, cell locations and cell lineage. Since our approach estimates the number of cells in each frame, their locations and the lineage tree, we report the following error metrics. Cell stage prediction: percentage of frames where the correct number of cells was predicted. Transition accuracy: number of frames between the ground-truth cell division and the predicted one. Localization: percentage of cells whose IoU with ground-truth is greater than 0.7. Lineage association: percentage of

Table 1. Cell stage prediction, cell transition (Trans.), localization (Loc.) and lineage reconstruction (Ling.) performance.

Experiments ($N_{max} = 5$)	Cell Stage Prediction (%)							Loc. (%)	Trans. Avg.	Ling. (%)	
	1-cell	2-cell	3-cell	4-cell	5-cell	Avg.	Overall			Ass.	Div.
Ours (MP)	100.0	99.6	95.5	91.7	88.2	95.0	95.5	74.2	4.0	74.0	81.7
Ours (JT)	100.0	99.6	95.5	91.8	88.2	95.0	95.6	82.6	4.0	80.8	86.0
Khan et al. [4]	100.0	99.6	95.5	88.7	88.2	94.4	94.6	—	6.4	—	—
<hr/>											
($N_{max} = 4$)											
Ours (MP)	99.8	98.8	80.9	99.1	—	94.6	98.8	76.9	1.9	76.3	83.1
Ours (JT)	99.8	98.8	80.9	99.1	—	94.6	98.8	86.0	1.9	93.2	89.8
Khan et al. [5]	99.1	99.5	43.3	98.9	—	85.2	97.9	87.0	2.8	92.9	86.4
Khan et al. [4]	99.8	98.8	80.9	99.1	—	94.7	98.8	—	1.9	—	—


Fig. 2. Lineage tree examples. Green lines: Ground truth. Blue lines: Reconstructed lineage tree. The dotted red lines represents the ground-truth transitions. From left to right: Two examples of abnormal division patterns; an example of normal division pattern; an example of cell associations at the time of division.

correctly estimated mother-daughter relationships. Lineage division: percentage of correctly predicted divisions, i.e., correct association when a division occurs.

The results of these different metrics are reported in Table 1. The top half of the table contains results for the case where $N_{max} = 5$, which represents the scenario where all known biomarkers can be computed, and where only our cell localization approach is applicable. The bottom half of the table corresponds to $N_{max} = 4$, and thus our lineage tree estimation technique was applied either to our cell localization technique, or as a post-processing step to the method of [5].

As can be observed from the table, our approach yields accurate lineage tree estimates. In particular, for $N_{max} = 4$, it yields better results when applied with our cell localization method than with the one of Aisha et al. [5]. Fig. 2 illustrates an example of cell associations and localization for 3-4 cell division. Mother and daughters are marked in yellow. Importantly, our approach was able to identify all the abnormal cell division patterns, some of which are illustrated in Fig. 2, where only one of the cells in the 2-cell stage further divides to yield the four cell stage. In terms of cell stage prediction, both our inference strategies (MP and JT) yield very similar and accurate results. Note that, for $N_{max} = 4$, our approach

yields much more accurate results than [5] for the 3-cell stage. Three cell periods tend to be very short and the hypotheses scoring function of [5] performs poorly here, which can be improved with more discriminating features. Importantly, this stage is crucial for the accuracy of the second and third timing biomarkers. For the cell transition accuracy, our approach also outperforms the results of [4] (for $N_{max} = 5$) and [5] (for $N_{max} = 4$). Finally, in terms of localization, our JT inference yields more accurate results than the MP one, and are similar to [5] (for $N_{max} = 4$). The running time of inference with JT and MP is 5 hours and 1 hour per sequence, respectively, which is within the frame rate (300s).

4 Conclusion

We have presented an automated approach to identify abnormal division patterns in developing human embryos by performing lineage tree analysis. Our approach can be used in any model that can localize individual cells. Since existing models are either limited to the 4-cell stage or do not localize cells, we have also proposed a cell localization method that handles up to the 5-cell stage. Our results have shown that we can reliably identify abnormality in divisions and also detect and localize individual cells. Our approach therefore provides biologists with a tool to assist them in the embryo selection process, and, we believe, constitutes an important step towards understanding the human embryo development process. In the future we plan to automate the identification of other abnormalities in growing embryos, such as cell reabsorption and fragmentation.

References

1. Amat, F., Lemon, W., Mossing, D.P., McDole, K., Wan, Y., Branson, K., Myers, E.W., Keller, P.J.: Fast, accurate reconstruction of cell lineages from large-scale fluorescence microscopy data. *Nature Methods* (2014)
2. Chen, A.A., Tan, L., Suraj, V., Pera, R.R., Shen, S.: Biomarkers identified with TL imaging: discovery, validation, and practical app. *Fertility and Sterility* (2013)
3. El-Labban, A., Zisserman, A., Toyoda, Y., Bird, A.W., Hyman, A.: Discriminative semi-markov models for automated mitotic phase labelling. In: *ISBI* (2012)
4. Khan, A., Gould, S., Salzmänn, M.: Automated monitoring of human embryonic cells up to the 5-cell stage in time-lapse microscopy images. In: *ISBI* (2015)
5. Khan, A., Gould, S., Salzmänn, M.: A linear chain markov model for detection and localization of cells in early stage embryo development. In: *WACV* (2015)
6. Li, K., Miller, E., Chen, M., Kanade, T., Weiss, L., Campbell, P.: Computer vision tracking of stemness. In: *ISBI* (2008)
7. Liu, A.-A., Li, K., Kanade, T.: Mitosis sequence detection using hidden conditional random fields. In: *ISBI* (2010)
8. Lou, X., Hamprecht, F.: Structured learning for cell tracking. In: *NIPS* (2011)
9. Meseguer, M., Herrero, J., Tejera, A., Hilligse, K.M., Ramsing, N.B., Jose, R.: The use of morphokinetics as a predictor of embryo implantation. *HR* (2011)
10. Moussavi, F., Yu, W., Lorenzen, P., Oakley, J., Russakoff, D., Gould, S.: A unified graphical models framework for automated mitosis detection in human embryos. *IEEE Trans. Med. Imaging* 1551–1562 (2014)

11. Schiegg, M., Hanslovsky, P., Kausler, B.X., Hufnagel, L., Hamprecht, F.A.: Conservation tracking. In: ICCV (2013)
12. Wang, Y., Moussavi, F., Lorenzen, P.: Automated embryo stage classification in TLM video of early human embryo development. In: MICCAI (2013)
13. Wong, C., Loewke, K., Bossert, N., Behr, B., Jonge, C.D., Baer, T., Pera, R.R.: Non-invasive imaging of human embryos before embryonic genome activation predicts development to the blastocyst stage. *Nature Bio.* (2010)
14. Yang, F., Mackey, M.A., Ianzini, F., Gallardo, G., Sonka, M.: Cell segmentation, tracking, and mitosis detection using temporal context. In: Duncan, J.S., Gerig, G. (eds.) MICCAI 2005. LNCS, vol. 3749, pp. 302–309. Springer, Heidelberg (2005)